Geometry influence on the transmission spectra of dielectric single layers of spheres with different compactness

A. Andueza, R. Echeverría, P. Morales, and J. Sevilla

Citation: Journal of Applied Physics **107**, 124902 (2010); doi: 10.1063/1.3434529
View online: https://doi.org/10.1063/1.3434529
View Table of Contents: http://aip.scitation.org/toc/jap/107/12
Published by the American Institute of Physics

Geometry influence on the transmission spectra of dielectric single layers of spheres with different compactness

A. Andueza, R. Echeverría, P. Morales, and J. Sevilla[a)]
Department of Electric and Electronic Engineering, Universidad Pública de Navarra, 31006 Pamplona, Spain

(Received 6 March 2010; accepted 28 April 2010; published online 16 June 2010)

The transmission of spectra of different dielectric spheres single layer arrangements has been measured. High dielectric permittivity ($\varepsilon=7$) spheres of several millimeters of diameter were used to build the samples whose transmission was measured in the microwave range. The behavior of lattices arranged in square and triangular geometries have been compared in a number of different compactness cases. The same patterns measured have also been calculated by finite-difference time-domain (FDTD) method. Spectra from different geometrical arrangements of the same compactness (measured with the same filling fraction value) are very similar in some cases. Based on the level of similarity we propose three compactness regions. The high compactness region, where the structure effect is important, presents spectra clearly different for the two geometries. In a medium compactness region spectra are almost identical, suggesting a dominant effect of single sphere effects. Finally, in the low compactness region, the spectra from the two geometrical configurations diverge again as the Bragg diffraction values are approached. © *2010 American Institute of Physics*. [doi:10.1063/1.3434529]

I. INTRODUCTION

Photonic crystals (PhCs) (Refs. 1–3) are very promising materials for future telecommunication devices because of their capacity to control electromagnetic waves. This control is due to the photonic band gap (PBG),[4] which may appear for PhCs in some particular arrangements, thereby, preventing light from propagating through the crystal. The presence of a PBG in PhC structures can give rise to phenomena similar to those of semiconductors in electronics, such as wave guiding, optical switching, or optical filtering.

Periodic arrangements of dielectric spheres[5–23] give the possibility of creating ultracompact and efficient photonic devices at low cost, using techniques such as opal self-organization.[5–9] At present time, high quality bare opals are obtained by using spheres of polymethylmethacrylate (PMMA) or silica (SiO_2), materials that exhibit quite low refractive indices. However, the use of higher refractive index materials could open new possibilities in designing more efficient photonic devices, and toward this aim, a couple of experimental methods have been developed to synthesize higher refractive index spheres. For example, recent studies report the synthesis of titania (TiO_2) spheres with diameters of a few hundreds nanometers with coefficients of variations in size ranging from 5% to 20% and refractive indices as high as 2.9.[12,13] It is easy to imagine the use of other materials in order to reach high refractive indices.

Single layers of dielectric spheres have received increasing attention recently.[13–20] Such structures can be used as planar defects in three-dimensional (3D) structures[21] or as building blocks for the creation of two-dimensional (2D)/3D hybrid architectures, for instance. Improved fabrication techniques allow specific patterns to be engineered in such monolayers by using micromanipulation,[13] electron beam lithography,[22] or laser-induced breakdown.[23] These novel techniques, currently adapted to PMMA and SiO_2 spheres in particular, enable the design of new PhC structures that may exhibit very useful properties. One can expect that similar techniques will be adaptable to higher refractive index spheres in the near future.

Spheres are well-defined resonators that can be regarded as the photonic version of individual atoms in electronic crystals.[13] It is generally accepted that a photon in an isolated dielectric sphere is trapped like an electron in an atom. However, this confined photon can hop from one sphere to the neighbor by the optical tunnel effect. This coherent motion of the photon in the periodic lattice gives rise to the photonic band.[16] Thus, the band origin can be regarded as double such as: caused by Mie scattering by individual spheres in one hand and by Bragg resonances from the periodic arrangement in the other.[13]

The aim of this work is to investigate the influence in the electromagnetic transmission spectra of dielectric spheres single layers of the geometrical disposition of the spheres. The experiments were performed in the microwave regime because the structures are much easier to be built with spheres of several millimeters, while the physical behavior should be the same due the scaling properties of Maxwell equations. Several single layers were thus constructed in the two possible symmetric arrangements, triangular and square, for different values of compactness. The transmission spectra of these samples were measured and also numerically calculated by FDTD method.

The obtained results are discussed having in mind the map of resonances frequency against compactness,[19] comparing the transmission spectra with the calculated Mie resonances for individual spheres and with the first-orders Bragg diffraction. The most interesting result is the extraordinary

[a)]Author to whom correspondence should be addressed. Tel.: (34) 948 16 92 75. FAX: (34) 948 16 97 20. Electronic mail: joaquin.sevilla@unavarra.es.

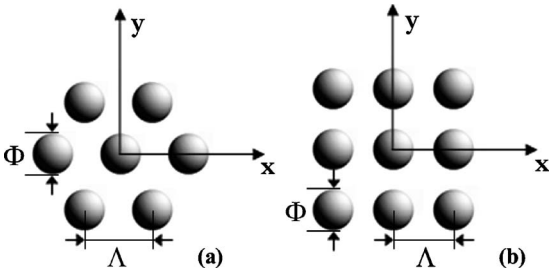

FIG. 1. Geometrical arrangements used (triangular and square, respectively) and parameters definition.

similarity of the spectra obtained from lattices of medium compactness values. As the layers become more compact, the arrangement geometry becomes more relevant. In the low compactness region, only one to two resonances remain matched, increasing the geometry influence as the first-order Bragg diffraction value is approached. Therefore, three compactness regions can be identified regarding the influence of the geometry in the transmission spectra.

II. EXPERIMENTAL

Spherical soda lime glass spheres provided by Afora SA were used. The spheres have a high dielectric permittivity $\varepsilon=7.0$ ($n=2.65$) in the frequency range considered for the measurements, which extends from 10 to 30 GHz. Sphericity and monodispersion of spheres were good, nonuniformity of diameter was measured to be less than 1% of the nominal value.

The lattice geometries used were triangular and square, with a parameter notation shown in Fig. 1; we will use Φ for the sphere diameter and Λ to refer to the lattice constant, the separation between two consecutive centers in the unit cell.

A simple parameter to indicate the compactness of a particular arrangement is the ratio Φ/Λ, denoted by R in the following. However, in order to compare, we need a parameter describing the layer compactness for both lattices. This parameter is the filling factor, denoted by ff. Filling factor is defined as the volume fraction that is occupied by spheres with respect to the total volume of a unit cell where the height equals the diameter of the sphere. Both parameters R and ff are geometrically related, therefore, we can calculate filling factor of the triangular (ff_t) and square lattice (ff_s) as

$$ff_t = \frac{\pi}{3\sqrt{3}}R_t^2, \tag{1}$$

$$ff_s = \frac{\pi}{6}R_s^2. \tag{2}$$

Spheres were held at their assigned positions by gravity, placing them on a surface of cardboard with smooth marks in each site as was shown in Fig. 2.

The values of Φ and Λ were selected for each R value in a convenient way, fixing the similar filling factor and diameter of spheres in both lattices and modifying the lattice period to match the structures. Therefore, the design election takes the higher benefit of our frequency window of measurement. Sphere diameters used were 7 and 8 mm.

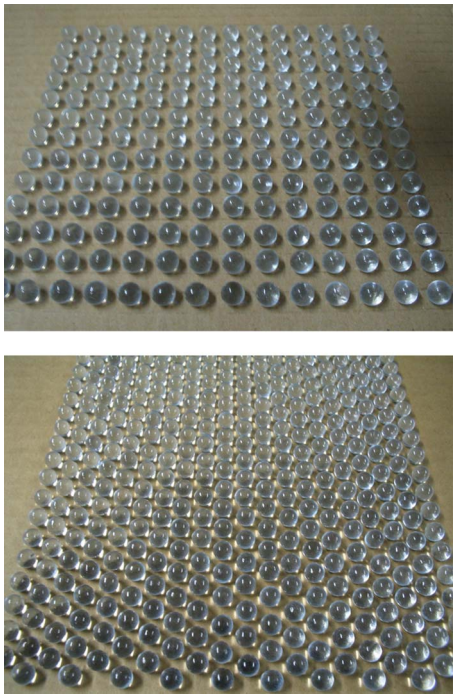

FIG. 2. (Color online) Photography of the single layers of glass spheres used in the measurements for square and triangular lattices, respectively.

The transmission spectra of these structures were measured by using a network analyzer (HP 8722ES), spliced to rectangular horn antennas 60×40 mm^2 (Narda Model 639), aligned in the z direction, separated 300 mm approximately from each other. In the middle of this space the sphere arrangements were placed perpendicular to the antennas axis. Spectra where registered using differential measurement technique to enhanced the frequency response of the antennas.

Computer calculations were carried out using the CST MICROWAVE STUDIO™, a commercial code based on the finite-integration time-domain method. This program is an electromagnetic field simulation software package specially suited for analysis and design in the high-frequency range. In our simulations absorption effects were neglected, remaining for the sphere material characterization only the dielectric permittivity, fixed always as $\varepsilon=7.0$

III. EXPERIMENTAL RESULTS AND DISCUSSION

Following the above described experimental procedure, transmission spectra were measured for triangular and square lattices for seven values of compactness in each case. The selected values for the filling factor were $ff=0.532$, 0.47, 0.41, 0.295, 0.23, 0.16, and 0.10, scanning every region of mode map;[19] high (0.532, 0.47, and 0.41), medium (0.295, 0.23, and 0.16), and low (0.1).

Figures 3–5 show the transmission spectra of the sphere arrays. The plots from the square and the triangular lattices are always presented together, with solid line the first and with dashed line the triangular. In all cases two figures are presented together, being the one in the left the corresponding to FDTD calculations and the one in the right the experimental measurements. Besides the spectra, the frequency

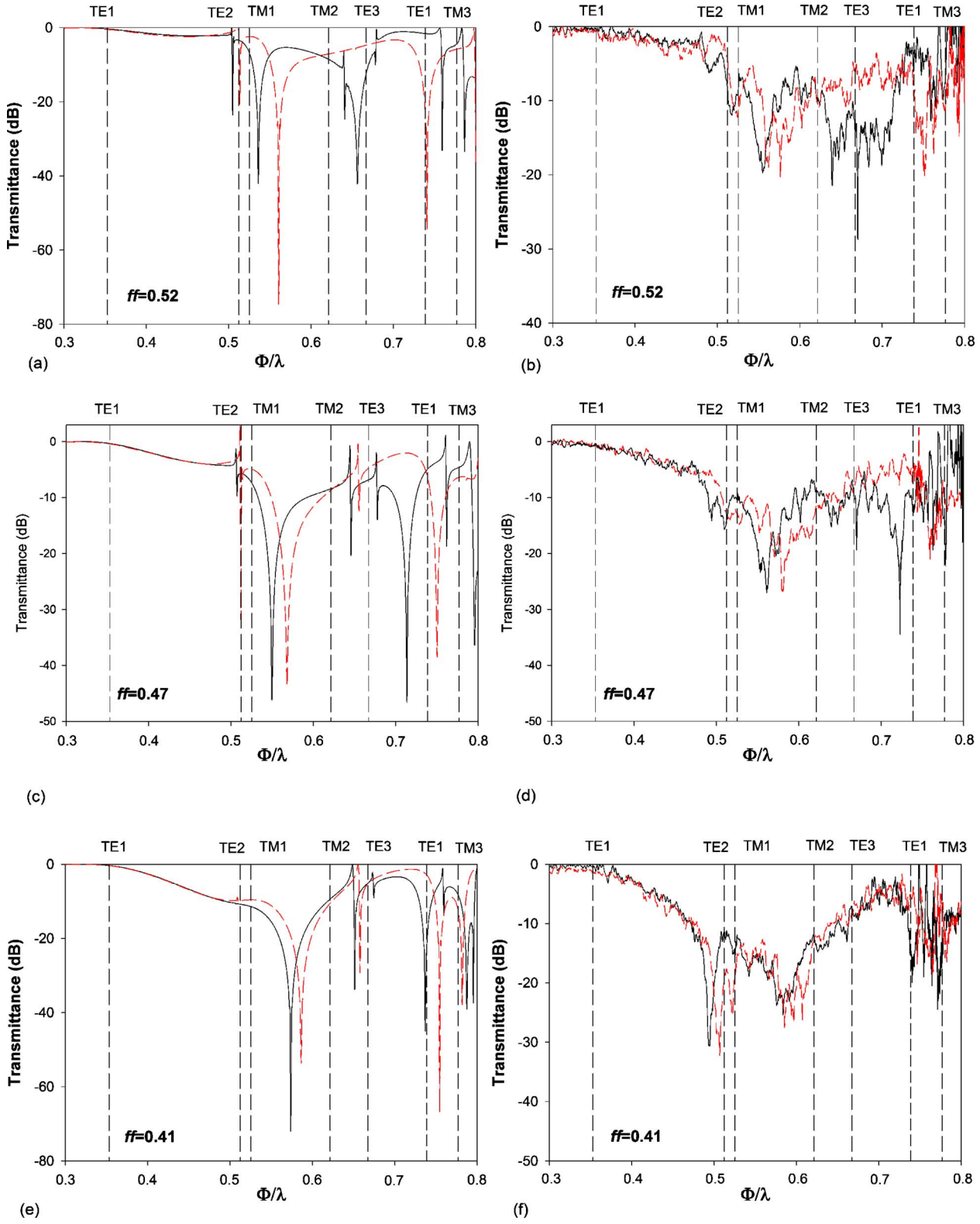

FIG. 3. (Color online) Transmission spectra of lattices with $ff=0.523$ (a) and (b), $ff=0.47$ (c) and (d), $ff=0.41$ (e) and (f). In all figures the two lines stand for the square lattice (solid) and the triangular one (dashed). Figures in the left (a), (c), and (e) show FDTD calculations, and the rest measurements.

values corresponding to the single sphere Mie resonances[24] are shown at the top of the figures. As the frequency values in the plots are presented normalized to sphere size (λ/Φ), their values remain constant for both lattices, resulting in vertical lines. In the case of measured spectra, the overlapping of noise begins to be significant, in some cases, for values of normalized frequency (λ/Φ) higher than 0.75, making difficult to identify fine measurements.

Figure 3 shows the calculated and measured spectra corresponding to the higher compactness region, with ff of 0.532, 0.47, and 0.41. The agreement between the FDTD numerical calculations and the experimental values is good

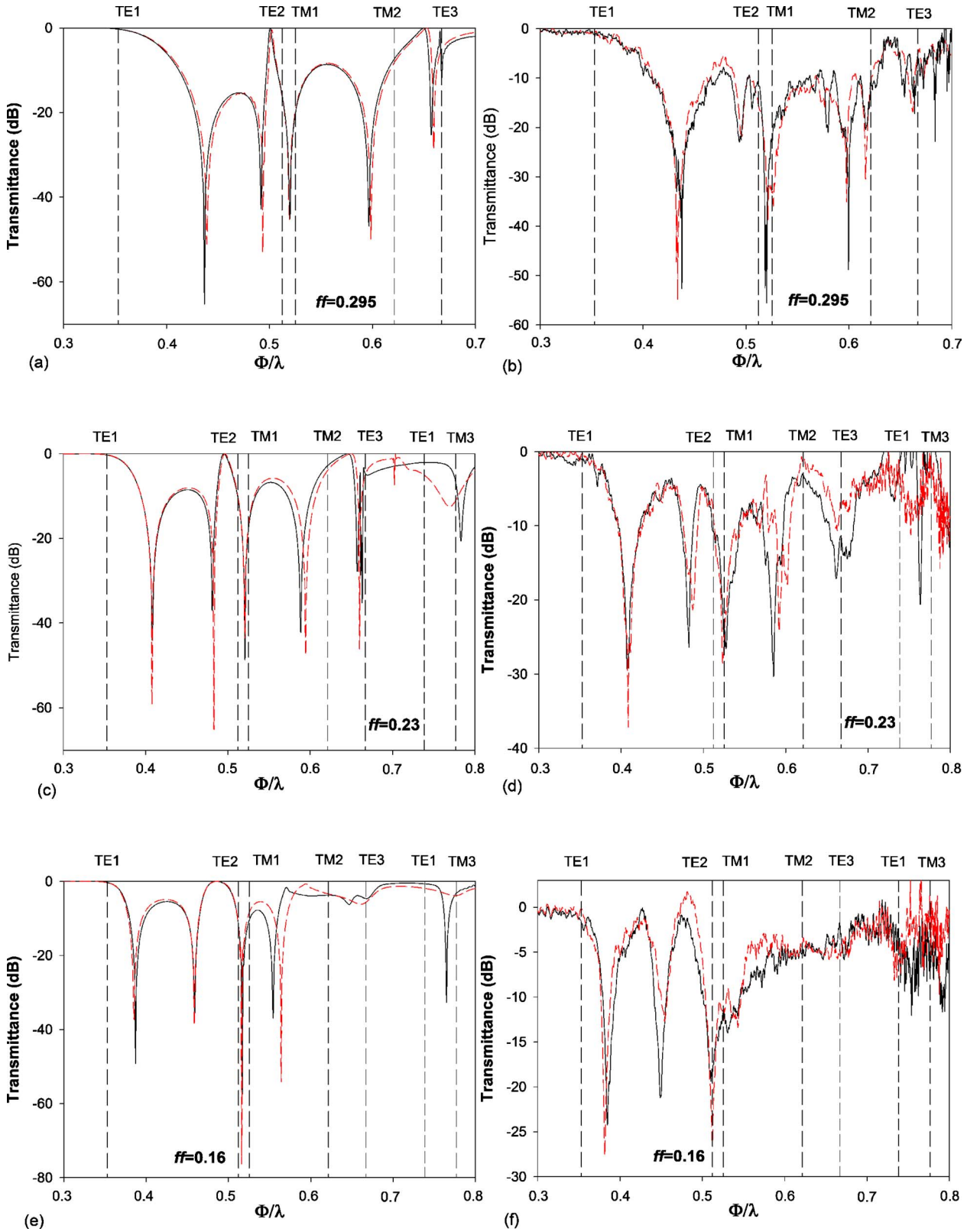

FIG. 4. (Color online) Transmission spectra of lattices with $ff=0.295$ (a) and (b), $ff=0.23$ (c) and (d), $ff=0.16$ (e) and (f). In all figures the two lines stand for the square lattice (solid) and the triangular one (dashed). Figures in the left (a), (c), and (e) show FDTD calculations, and the rest measurements.

in general. The largest discrepancy happens in the $ff=0.41$ case, where an experimental dip around $\lambda/\Phi=0.59$ is not predicted by the calculation.

On the other hand, significant variations are found when comparing square and triangular lattices. Especially remarkable is the mismatch in the position of the dips in the spectra for $ff=0.52$ and $ff=0.47$ [see Figs. 3(a)–3(d)], where only the first resonance seems to be related. Moreover, the results suggest the dependence of this resonance with the TE2 Mie mode independent of the ff. In Fig. 3(e), the first dip, close

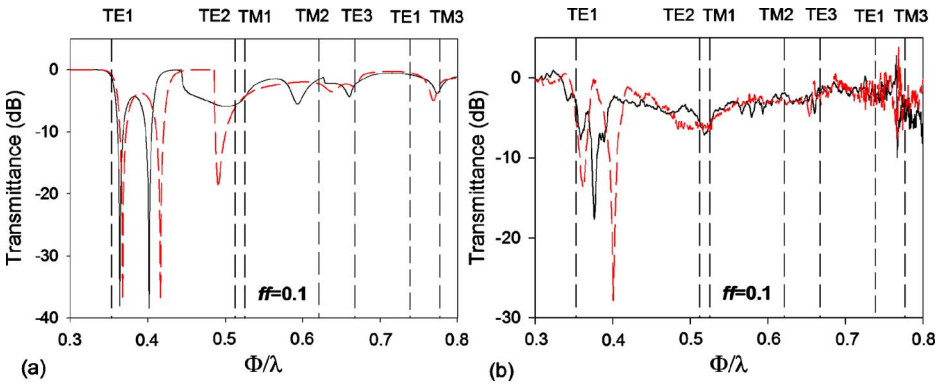

FIG. 5. (Color online) Transmission spectra of lattices with $ff=0.1$. The two lines stand for the square lattice (solid) and the triangular one (dashed). Figures (a) show FDTD calculations and (b) experimental measurements.

to Mie resonance TE2, is practically imperceptible in the triangular lattice and is not found for the square lattice for the calculated spectra, however, a deep peaks appear in the measurement for both lattices [Fig. 3(f)].

Broadband dips around the frequency of 0.59 are present both in the calculations and in the measurement. The sharpness and depth of these dips is different for the two geometries considered but is clear the correspondence between them. A third dip is found in the calculated spectra for $\lambda/\Phi=0.58$, around TE3 Mie resonance. However it is only present in measurement spectra of the square lattices for $ff=0.52$ and $ff=0.47$. The final zone of the measurement spectra is not clear due to the background noise added, therefore, it has not been possible to resolve the electromagnetic behavior of the lattices.

Besides the previous discussion on peak positions, as a general consideration about the three compactness value spectra, we see a clear increase in the similarity between the spectra of the triangular and the square lattices as ff decreases. This likehood increase can be seen both in the calculated and in the measured spectra. As we can see in Fig. 4, this tendency reaches a maximum in the medium compactness region, where triangular and square lattices present the same behavior for low order resonances.

Numerical and experimental transmission data corresponding to medium compactness region ($ff=0.295$, $ff=0.23$, and $ff=0.16$) are shown as a function of normalized frequency Φ/λ in Fig. 4, for both lattices. The agreement between experimental and calculated data is very good, not only in the frequency position of the dips but also in width and almost in depth. Even more remarkable is the similarity between the results obtained from the two studied lattices. For this range of compactness values the transmission spectra of triangular and square lattices are identical.

The higher discrepancy between both lattices is found in the fourth peak ($\Phi/\lambda=0,55$) of the $ff=0.16$ case. It is also the only place with appreciable difference between calculated and measured results: a clear dip in the calculation is only insinuated in the measurement.

We can observe how the second and third resonances in the Fig. 4 (also in Fig. 5) are close of TM1 and TE2 Mie resonances of isolated sphere in every ff cases study but this proximity slightly varies from one compactness value to other. Similar behavior can be observed also in the Fig. 4 around the TE3, TM2, and TM3 Mie modes. These correspondences suggest that the characteristics of Mie resonances for an isolated sphere indeed appear in the transmission spectra, representing a significant influence in the observed response. A behavior clearly dominated by isolated sphere modes would be the easiest explanation for the extraordinary agreement found between triangular and square lattices data. Nevertheless, the layer resonances are close but not matching the Mie resonance frequencies.

A slightly more complicated approximation would be to consider the effect of the environment on a single sphere as an average leading to some kind of effective dielectric permittivity. This would also be nice because the matching between triangular and square data happens for the same filling factor values. We have tried several *ad hoc* effective values for the dielectric permittivity of the medium surrounding a sphere finding worse matching in all cases. A variation in the dielectric permittivity shifts all the low order Mie resonances in the same direction, either to higher or lower frequency values. As the proximity between Mie resonances and experimental dips appears in different direction in different cases, it is evident that this idea cannot work.

We should then conclude that the Mie resonances do play a significant role in the building up of the collective modes of spheres single layers but not in a straightforward way. Some influence of the environment shift the exact values of the resonance frequencies, although for this compactness vales, in the same way for triangular and square arrangements.

Finally the transmission spectra for square and triangular lattice $ff=0.1$ is shown in Fig. 5 as well as the numerical result. The spectra present two sharp dents followed, at higher frequencies by shallower variations. The first dip corresponds with the lower frequency Mie resonance, TE1, and is almost identical for both geometrical configurations. The second dip, around $\Phi/\lambda=0.4$, present a significant variation for the two lattices, and the same happens for the rest of the spectra, similar accidents but not exact neither at the same frequency values are present.

Although the influence of the Mie modes in the system behavior is important, the exact coincidence of the first peak in Fig. 5 with the TE1 mode is somehow accidental, as can be realized from Fig. 6. For the triangular lattice we see in Fig. 6(a) that the lowest frequency dip crosses the TE1 value for a compactness of $ff=0.10$, therefore, if we consider other values of ff the coincidence would not be so precise. However, the precise matching of the observed value for this peak between the triangular and the square lattices does takes

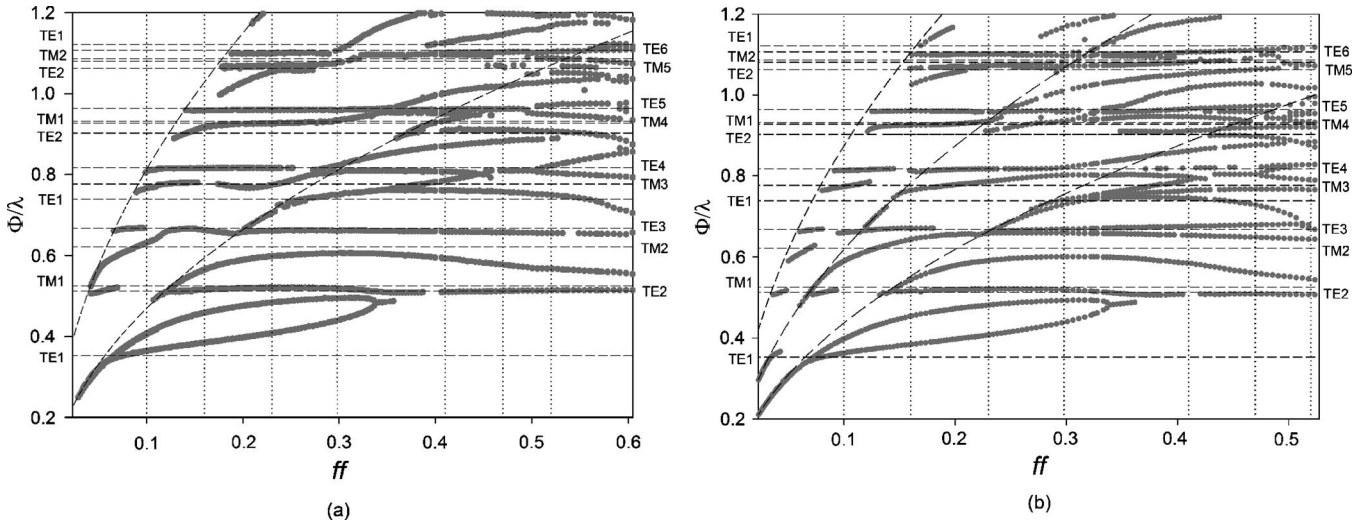

FIG. 6. Mode maps of 2D arrays of dielectric spheres in triangular (a) and square (b) arrangements at normal incidence.

place for all ff values in this range. The complete coincidence between spectra of the square and the triangular lattices shown for $ff=1.16$ [see Figs. 4(e) and 4(f)] starts to disappear smoothly except for the lowest frequency peak, where the coincidence remains in all the cases we have studied.

It is interesting to note that the discrepancy appears for the resonance when it is close to the Bragg diffraction value. The high-frequency dent is relatively close to the Bragg diffraction line for $ff=0.1$, as can be better appreciated in Fig. 6. The same happen in the case of the fourth peak in the $ff=0.16$ data [Figs. 4(e) and 4(f)] above mentioned. These data suggest that the resonances taking place close to the Bragg diffraction frequency are more affected by the structure. Square and triangular lattices with the same filling factor, as the sphere diameter is also equal, have different values of the lattice constant Λ. Therefore, the frequency of the Bragg diffraction is not the same for both lattices. This could be an explanation for the observation of increased discrepancy between square and triangular lattices for peaks close to Bragg diffraction values.

In order to get a more integrated view of the spectra features of different compactness values the representation shown in Fig. 6 is presented. In this plot, previously included in Ref. 19 for triangular lattices, we present the resonance frequency values for each compactness case. The plotted values are obtained from the simulation, what allows more precise data (for many more compactness values) and a range extension that is very interesting for the discussion. The measurement range ends below $\Phi/\lambda=0.8$ as previously stated because of an increase in the noise level (due to limitations in the antennas); however, in the simulation spectra peaks can be clearly identified up to $\Phi/\lambda=1.2$. The frequency values of the lowest order Mie resonances, and the measured samples, are also presented in the plot as horizontal and vertical lines, respectively. As data are presented normalized to sphere diameter, the Mie resonances are not affected by the lattice compactness. Finally, the sloped curves represent the first-orders Bragg diffraction.[19] This map was used to select the seven values of compactness previously discussed.

This global visualization of the single layer nontransmission frequencies together with the Mie modes and the Bragg values allows further discussion. The general similarity between the triangular [Fig. 6(a)] and the square [Fig. 6(b)] cases is clear.

The Mie modes are only dependent on the sphere radius (and the dielectrical permittivity, that is held constant in all cases), and, therefore, both lattices share the frequency values of this resonances. This is not the case for the Bragg frequencies. The Bragg condition depends on the intersphere separation Λ (see Fig. 1), and for the same filling factor value we do not have the same Λ. As can be easily seen from Eqs. (1) and (2), $\Lambda_t \neq \Lambda_s$. In the triangular case successive Bragg scattering frequencies take place at integer number of times Λ_t. In the square case there are two families of frequencies for the Bragg scattering, those produced by the nearest neighbors (at a distance Λ_t) and those produced by the second order neighbors, at $\sqrt{2}\cdot\Lambda_t$. In Fig. 6(a) two lines are present corresponding to the first Bragg orders, and in Fig. 6(b) we see again the first two corresponding to the nearest neighbors and, in between, the first corresponding to second order neighbors.

Some of the lattice resonances keep present very close to Mie ones for long intervals of compactness values. This is the case of the lowest frequency peak for highest compactness value, close to TE2-TM1, and of the third one, close to TE3. Other Mie modes seem to be modified by the structure, and significantly affected by its compactness. This would be the case of the two lowest frequency peaks (the ones appearing for filling factor values below 0.35) or the one above the TE2-TM1 lines. The line representing these modes in Fig. 6 bends when approaching the Bragg in such a way that they merge for low compactness values. It is not surprising then that the resonances close to the Bragg scattering frequencies appear at different positions for the two symmetries considered.

For high compactness values, at the right hand side of Fig. 6, some differences appear between the two considered lattices. The triangular one, being geometrically the most

compact possible, extends to higher values of filling factor. Lattice resonances at he highest comparable values of filling factor does not take place at identical positions as previously seen in spectra shown in Fig. 3.

Summarizing, we have seen how for highly compact lattices, *ff* over 0.5, the spectra from the two geometries is quite different but as compactness decreases they start to converge. For values of 0.47 and 0.41 the spectra from both lattices is very similar but shifted in frequencies, in the former case more than in the later. For medium compactness values (*ff* ranging from 0.3 to 0.15) the response of both geometries is remarkably close. This similarity is lost for the peaks approaching the Bragg diffraction values. Regarding these results, we can establish three different zones: a high compactness region, a near to Bragg diffraction region and a medium compactness no Bragg region.

For highly compacted lattices, as previously seen, the spectral features for both lattices are quite different. This could be due to a significant interaction between nearest spheres in the close packed (and nearly) system[15] because this nearest neighbors are different in each lattice. For these strong interactions it has been proposed the existence collective states generated from the combination of single sphere ones calculated by tight-binding method.[25] It has been reported that this tight-binding picture based on spheres resonances holds well in the single layer of dielectric spheres with a large refractive index.[16]

For highly diluted lattices the system is dominated by Bragg diffraction, as has been previously stated.[19] This leads to differences in the peak position of spectra from the two geometries because they present different nearest neighbors distance (and hence Bragg frequencies) for the same filling factor.

For the intermediate compactness values, we see an impressive similarity in the spectra from both geometries, what lead to think that the structure effect is negligible and that is the isolated sphere the dominating behavior in this region. However, although the dips are somehow near the Mie resonance values, the coincidence is not precise. The possibility of considering the Mie resonances of a sphere in an effective surrounding media taking into account homogeneous effects did not helped to improve the fitting. Further research is needed to elucidate if the resonance of the single layers in this region are some kind of frequency shifted Mie modes (and how the modification is produced) or if there are more complex interactions.

IV. CONCLUSIONS

The transmission spectra of high dielectric constant of $\varepsilon=7$ spheres has been measured and calculated for the two possible regular arrangements, square, and triangular, in a range of lattice compactness values (identified by their filling factor). The most striking conclusion is the perfect overlapping of the spectra from the two geometries found for certain filling factor values. From the analysis of the similarities among the spectra obtained from the two geometries, we propose three different regions and suggest the dominating physical effect in each one as follows:

(i) High compactness region (from close packed to lattice parameters around 25% larger than sphere diameter), where the sphere modes significantly overlap and the structure factor is relevant, leading to appreciable differences in the spectra. The resonances in this region could be due to tight-binding combinations of individual sphere modes.

(ii) Bragg diffraction region (all single layer resonances close to the first-order Bragg diffraction), where we find different frequency values in each lattice, suggesting that the effect of Bragg diffraction strongly affects these resonances. For very low compactness all resonances are close to Bragg diffraction values.

(iii) Medium compactness far from Bragg diffraction region, where the data obtained from square and triangular lattices are extremely similar. The effect of isolated sphere should be dominant but the discrepancy of the obtained values with the calculated Mie modes indicates some distortion introduced by the system that requires further investigation.

[1] E. Yablonovitch, Phys. Rev. Lett. **58**, 2059 (1987).
[2] S. John, Phys. Rev. Lett. **58**, 2486 (1987).
[3] *Photonic Cristal, Molding the Flow of Light*, edited by J. D. Joannopoulos, R. D. Meade, and J. N. Winn, (Princeton University Press, Princeton, New Jersey, 2005).
[4] *Photonic Band Gap Materials*, edited by C. M. Soukoulis (Kluwer Academic, Dordrecht, 1996).
[5] V. N. Bogomolov, S. V. Gaponenko, I. N. Germanenko, A. M. Kapitonov, E. P. Petrov, N. V. Gaponenko, A. V. Prokofiev, A. N. Ponyavina, N. I. Silvanovich, and S. M. Samoilovich, Phys. Rev. E **55**, 7619 (1997).
[6] J. E. G. J. Wijnhoven and W. L. Vos, Science **281**, 802 (1998).
[7] A. Blanco, E. Chomski, S. Grabtchak, M. Ibisate, S. John, S. W. Leonard, C. Lopez, F. Meseguer, H. Miguez, J. P. Mondla, G. A. Ozin, O. Toader, and H. M. Van Driel, Nature (London) **405**, 437 (2000).
[8] Y. A. Vlasov, X.-Z. Bo, J. C. Sturm, and D. J. Norris, Nature (London) **414**, 289 (2001).
[9] C. López, Adv. Mater. **15**, 1679 (2003).
[10] A. Reynolds, F. López-Tejeira, D. Cassagne, F. J. García-Vidal, C. Jouanin, and J. Sánchez-Dehesa, Phys. Rev. B **60**, 11422 (1999).
[11] X. Jiang, T. Herricks, and Y. Xia, Adv. Mater. **15**, 1205 (2003).
[12] E. Mine, M. Hirose, D. Nagao, Y. Kobayashi, and M. Konno, J. Colloid Interface Sci. **291**, 162 (2005).
[13] H. T. Miyazaki, H. Miyazaki, K. Ohtaka, and T. Sato, J. Appl. Phys. **87**, 7152 (2000).
[14] S. Yano, Y. Segawa, J. S. Bae, K. Mizuno, S. Yamaguchi, and K. Ohtaka, Phys. Rev. B **66**, 075119 (2002).
[15] Y. Kurokawa, Y. Jimba, and H. Miyazaki, Phys. Rev. B **70**, 155107 (2004).
[16] T. Kondo, M. Hangyo, S. Yamaguchi, S. Yano, Y. Segawa, and K. Ohtaka, Phys. Rev. B **66**, 033111 (2002).
[17] K. Ohtaka, Y. Suda, S. Nagano, T. Ueta, A. Imada, T. Koda, J. S. Bae, K. Mizuno, S. Yano, and Y. Segawa, Phys. Rev. B **61**, 5267 (2000).
[18] T. Kondo, S. Yamaguti, M. Hangyo, K. Yamamoto, Y. Segawa, and K. Ohtaka, Phys. Rev. B **70**, 235113 (2004).
[19] A. Andueza, R. Echeverría, and J. Sevilla, J. Appl. Phys. **104**, 043103 (2008).
[20] A. Andueza and J. Sevilla, Opt. Quantum Electron. **39**, 311 (2007).
[21] P. Massé, S. Reculusa, K. Clays, and S. Ravaine, Chem. Phys. Lett. **422**, 251 (2006).
[22] F. Jonsson, C. M. S. Torres, J. Seekamp, M. Schniedergers, A. Tiedemann, J. Ye, and R. Zentel, Microelectron. Eng. **78–79**, 429 (2005).
[23] W. Cai and R. Piestun, Appl. Phys. Lett. **88**, 111112 (2006).
[24] G. Mie, Zeitschrift für Chemie und Industrie der Kolloide **2**, 129 (1907).
[25] E. Lidorikis, M. M. Sigalas, E. N. Economou, and C. M. Soukoulis, Phys. Rev. Lett. **81**, 1405 (1998).